

Home-Made, Self-Powered, Skin-Attachable Sensing Platform for Diverse Vital Sign Monitoring

Xiaodong Wu,* Wenjuan Ren, Yuhan Wen, Seiya Ono, Juan Zhu, James W. Evans, and Ana C. Arias*

Cite This: *ACS Sens.* 2023, 8, 2740–2749

Read Online

ACCESS |



Metrics & More

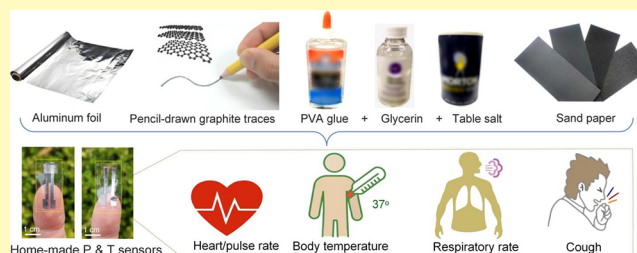


Article Recommendations



Supporting Information

ABSTRACT: Wearable electronic sensors that can perform real-time, continuous, and high-fidelity monitoring of diverse biophysical signals from the human body are burgeoning and exhibit great potential to transform traditional clinical healthcare. However, such emerging devices often suffer from strict requirements of special precursor materials and sophisticated fabrication procedures. Here, we present a new paradigm of a self-powered, skin-attachable, and multifunctional sensing platform that can be fully created just at home with daily necessities. Its operating mechanism is based on mechanical/thermal regulation of the potential difference output of a primary electrochemical cell. This



KEYWORDS: home-made sensor, mechanical sensor, thermal sensor, sensing platform, vital sign monitoring

Natural physiological processes of the human body yield a wide spectrum of vital signs (e.g., body temperature, cardiac rhythms, breathing, body motion, etc.). Continuous monitoring of these vital signs allows us to acquire valuable insights into our health status,^{1–4} promote the early warning and prevention of diseases (e.g., the early symptoms of COVID-19 infections are known as fever (98%), cough (65%), and shortness of breath (55%)^{5–7}), and define personalized treatment protocols that minimize morbidity and promote rehabilitation.^{8–10} Compared to the cumbersome, sophisticated, and expensive equipment used in the hospital, the emerging classes of body-integrated electronic sensors offer unique capabilities for accessing and evaluating these vital sign signals at home, making clinical healthcare more precise, safe, convenient, and efficient. Such home-centered health monitoring and diagnosis can be critically important, especially during the outbreak of an epidemic (e.g., COVID-19) when the medical resources in hospitals are limited or exhausted. Therefore, developing affordable and accessible platforms that enable home-centered healthcare and diagnosis is of tremendous significance.

Commercially available wearable electronics that measure physiological signals have been developed. Examples include Apple Watch, iRhythm, VitalConnect, Sibel Health, and so on. Nevertheless, the flexibility and adaptability of these standardized products for monitoring a diverse range of vital signs are

limited. Additionally, the affordability and accessibility of these nascent products cannot be guaranteed especially in an emergency (e.g., outbreak of serious epidemic). On the other hand, remarkable progress in wearable sensors has been achieved in academic research. However, by far, the vast majority of lab-created wearable sensors necessitates professional lab equipment and special precursor materials. For example, the well-established fabrication procedures of wearable sensors usually involve spin-coating, photolithography, wet/dry etching, and vacuum deposition.^{11–15} These procedures require harsh laboratory conditions and are energy- and time-consuming. The mostly used precursor materials for fabricating wearable sensors (e.g., metal nanomaterials, carbon nanomaterials, semiconducting polymers, and novel 2D nanomaterials) often suffer from high cost, limited disposability, and unproven bio-safety.^{16–20} Long-term contact with such nanomaterials may cause skin allergy, irritation, infection, or even cancer, posing a threat to human health. In addition, most of the commercialized

Received: April 1, 2023

Accepted: June 13, 2023

Published: June 22, 2023



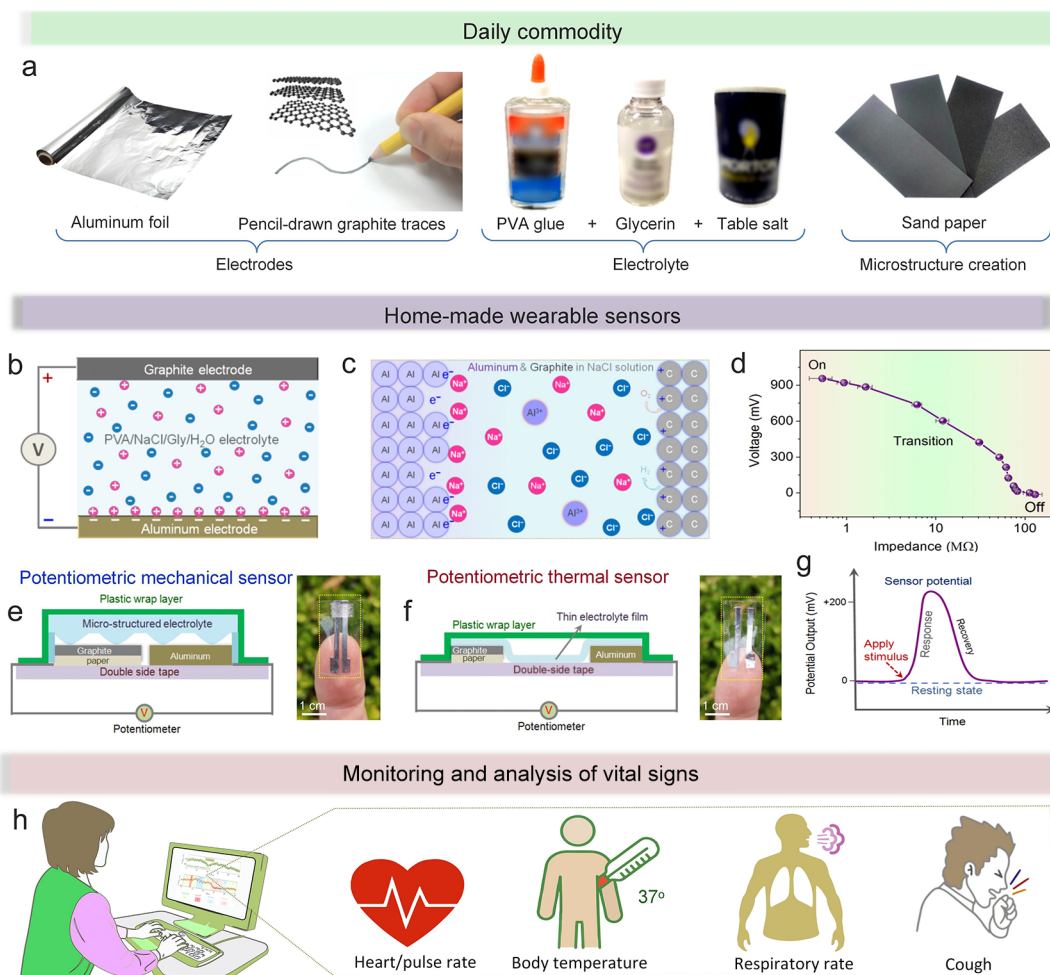


Figure 1. Design of the home-made sensing platform. (a) Pictures showing the selected daily commodities for preparing the proposed sensing platform. (b) Schematic illustrating that a potential difference can be created between the Al electrode and graphite electrode when they are in contact with a NaCl electrolyte. (c) Illustration showing the Al/electrolyte and graphite/electrolyte interfaces. (d) Relevance between the internal impedance and the potential difference output measured between the two electrodes. (e and f) Structural layouts and photographs of the potentiometric mechanical sensors and thermal sensors. (g) Diagram depicting that a sensor signal variation can be triggered by an externally applied mechanical or thermal stimulation. (h) Conceptual illustrations showing that diverse vital signs, such as heart/pulse rate, respiration rate, body temperature, and coughing, can be continuously monitored with the proposed home-made sensing platform.

sensors and lab-created sensors are power-hungry during continuous operation. The power consumption could reach as high as tens of mW per single device,²¹ which greatly restricts their long-term usage and widespread deployment. Motivated by these challenges, an appealing idea arises: can we substitute all of the precursor materials of the state-of-the-art wearable sensors with household necessities and develop a home-fabrication methodology for a powerful sensing platform that enables us to monitor diverse vital signs continuously, which, however, has never been explored so far?

Here, we systematically present the design concept, materials selection, operation mechanism, device structure, and fabrication method of a novel class of home-made and self-powered sensing platforms that enable us to monitor diverse vital signs continuously. The core working mechanism of this sensing platform is based on the stimulation-regulated variations in potential difference output of an electrochemical cell with an aluminum electrode, a graphite carbon electrode, and a sodium chloride (NaCl)-containing electrolyte. Through careful materials research, component tuning, and structural engineering, the externally applied mechanical stimulation (i.e., pressure,

force) and thermal stimulation (i.e., temperature) can be successfully encoded into the potential difference output of this sensing platform. Such a home-made sensing platform exhibits a number of distinguished characteristics, such as both mechano-transduction and thermotransduction capabilities, good signal compatibility, totally self-powered signal output, simplified operation/measurement, high cost-efficiency and energy-efficiency, good disposability and bio-safety, as well as superior customerization flexibility. Based on this proposed sensing platform, a wide spectrum of physiological vital signs, including body temperature, heart/pulse rate, respiratory rate, coughing, and diverse body motions, can be monitored continuously and analyzed in real time. This totally home-conducted design, fabrication, and utilization of wearable healthcare devices open up new opportunities for the broad adoption and extensive application of body-integrated smart electronics, with significant potential for societal benefits.

RESULTS AND DISCUSSION

Design of a Home-Made and Self-Powered Sensing Platform. To create a multifunctional sensing platform with

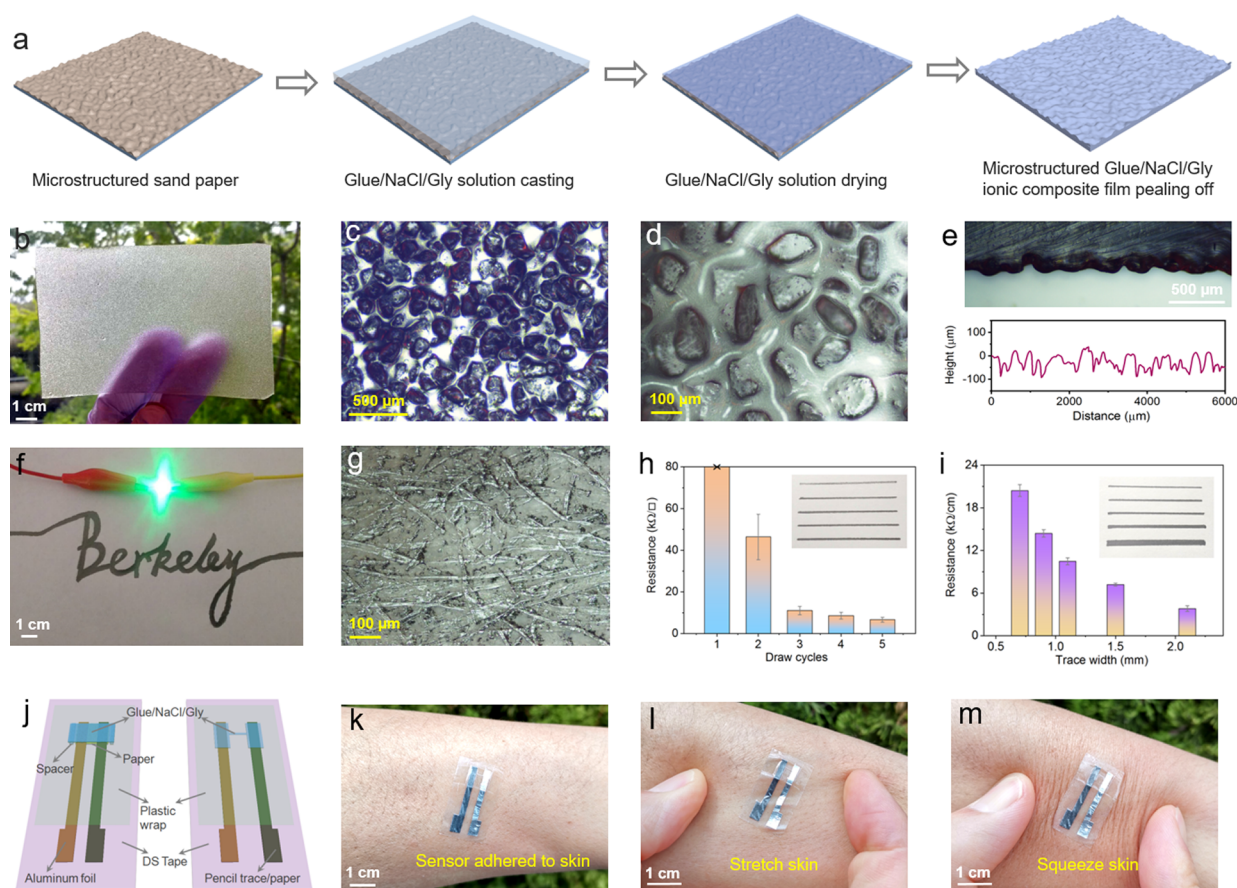


Figure 2. Fabrication of home-made skin-attachable sensors. (a) Schematic showing the creation of microstructure on the glue/Gly/NaCl electrolyte surface via a sandpaper molding strategy. (b–e) Photograph, optical microscopy images, cross-sectional image, and surface profile of the glue/Gly/NaCl electrolyte. (f) Picture showing the desired conductivity of the pencil-drawn patterns. (g) Microscopy image showing the interconnected graphite networks in the pencil traces. (h, i) Influence of the drawing cycle and trace width on the resistance of the pencil traces. (j) Illustration depicting the structural layouts of the potentiometric mechanical sensors and thermal sensors. (k–m) Pictures showing that a home-made sensor attached to planar skin, stretched skin, and squeezed skin, respectively.

household necessities, rational materials selection, component optimization, and structural engineering are crucial. Here, we choose aluminum (Al) foil and pencil traces (i.e., conductive graphite carbon) drawn on office copy papers as the two electrode materials (Figure 1a). Then, student glue (i.e., polyvinyl alcohol solution as the polymer matrix), glycerin (Gly) skin lotion (as the humectants and sensor performance regulator), and table salt (i.e., NaCl as the ion source) are carefully selected to prepare the electrolyte. Microstructures are created on the electrolyte surface via a sandpaper molding strategy for fabricating the mechanical sensors. All of these precursor materials are easily available with low cost (Tables S1 and S2), and the whole fabrication procedure can be accomplished just at home.

The working mechanism of this proposed sensing platform relies on a potentiometric sensing scheme. Specifically, an electric potential difference (≈ 900 mV) can be developed between the Al and graphite electrodes when they are in good contact with the NaCl-containing electrolyte (Figure 1b, see Figure S1 for detailed discussion). This is due to the fact that metallic Al is highly active and tends to dissociate into Al ions in a chloride environment, leaving abundant negative charges on the Al electrode surface (Figure 1c). For the chemically inert graphite electrode, there could be two possible reactions happening: oxygen reduction and/or hydrogen evolution.^{22,23}

These electrochemical reactions make this class of devices behave like a primary electrochemical cell. Interestingly, the potential difference output of such devices relies heavily on the internal impedance between the two electrodes, as presented in Figure 1d. This impedance-dependent potential difference output phenomenon makes it possible to encode external mechanical or thermal stimulations into the signal variation of the devices, resulting in a potentiometric mechanotransduction or thermotransduction mechanism.

The structural layout of the mechanical sensing device is shown in Figure 1e. A microstructured electrolyte with relatively high Gly content is placed on top of the Al and graphite electrodes. Applying a force/pressure will significantly regulate the interfacial impedance between the electrolyte and each of the two electrodes (Figure S2). The structural layout of the thermal sensing device is shown in Figure 1f. A thin electrolyte film with relatively low Gly content is attached on top of the two electrodes. The intrinsic impedance of this thin electrolyte film can be efficiently modulated by temperature variation (Figure S3). Leveraging these operating mechanisms and device configurations, a potential difference variation could be triggered by an externally applied mechanical or thermal stimulation (Figure 1g), which enables us to monitor a wide range of physiological vital signs, such as body temperature,

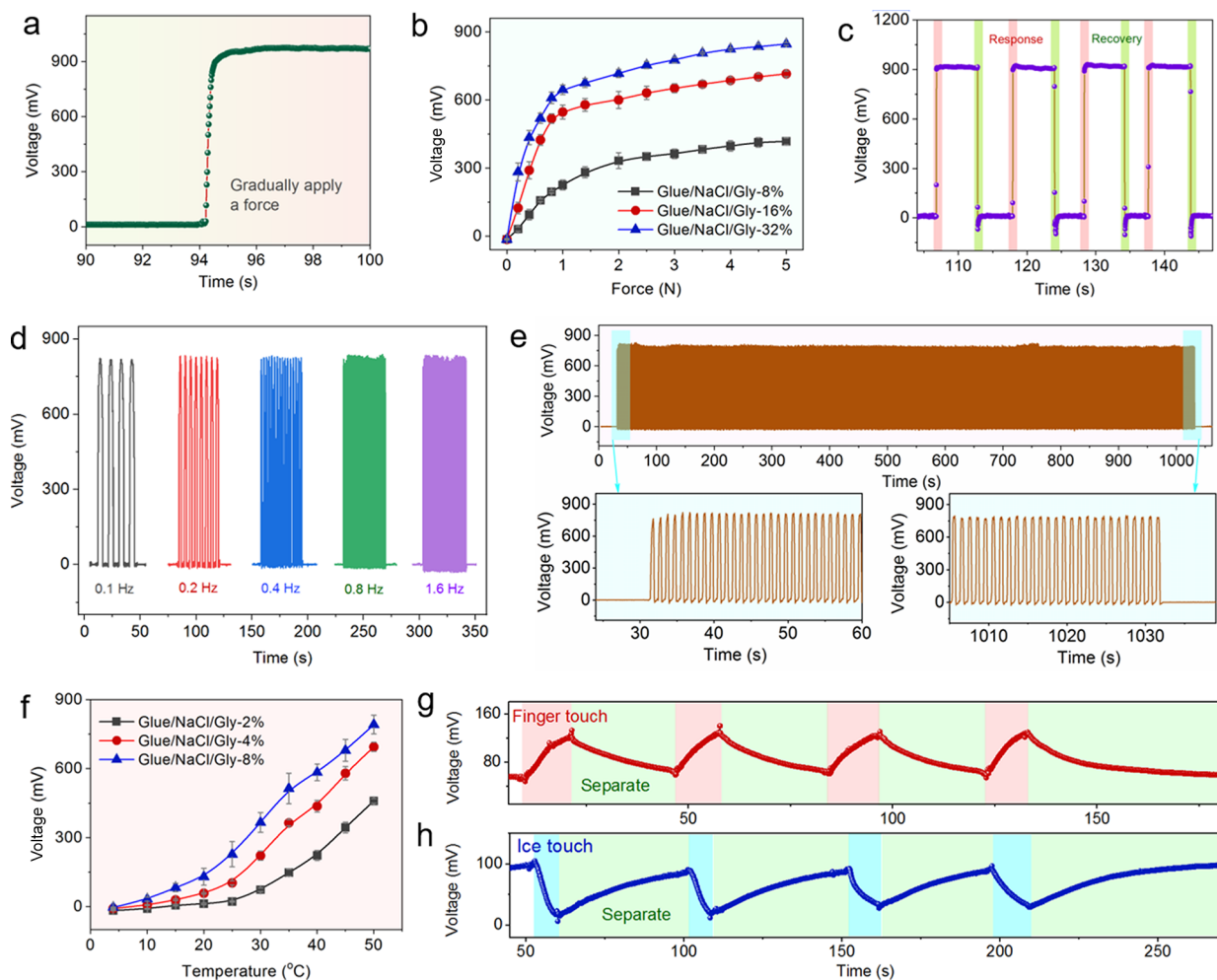


Figure 3. Performance of home-made sensors. (a) Continuous signal variation of a mechanical sensor when gradually applying a force on the device. (b) Response behaviors of mechanical sensors fabricated with different glue/Gly/NaCl electrolytes. Glue/Gly/NaCl- $X\%$ means that the weight ratio of Gly to the solid content of glue is $X\%$. (c) Response and recovery speeds of the mechanical sensors. (d) Responses of mechanical sensors to a force variation of varying frequency. (e) Repeatability and reproducibility of mechanical sensors in a cyclic test over 1000 cycles. (f) Performance of thermal sensors fabricated with different glue/Gly/NaCl electrolytes. Glue/Gly/NaCl- $X\%$ means that the weight ratio of Gly to the solid content of glue is $X\%$. (g, h) Response behaviors of the thermal sensors (at room temperature, $\approx 24\text{ }^{\circ}\text{C}$) to a warm finger ($\approx 31\text{ }^{\circ}\text{C}$) touch and a cold ice ($\approx 0\text{ }^{\circ}\text{C}$) touch repeatedly.

heart/pulse rate, respiratory rate, coughing, and body motions (Figure 1h).

Fabrication of a Home-Made Sensing Platform. The preparation process of the microstructured electrolyte is illustrated in Figure 2a. Glue/Gly/NaCl aqueous solutions are cast onto commercial sandpapers with rough surfaces. After drying the solution and peeling off the composites, semi-transparent glue/Gly/NaCl electrolyte films with uniform microstructures are fabricated (Figure 2b). The microstructure morphologies are presented in Figures 2c,d and S4. Spinosum surfaces with a random height distribution are observed, which stem from the templating effect of the sandpaper molds. The cross-sectional image and surface profile of the microstructured electrolyte (Figure 2e) also verify the rugged surface morphology. Such a microstructured surface of the electrolyte enables us to efficiently and continuously regulate the electrolyte/electrode interfacial impedance, thus achieving an effective and smooth mechanotransduction process.

An Al foil ($\approx 20\text{ }\mu\text{m}$) is cut into a defined geometry to serve as the Al electrode. To prepare the conductive graphite electrode, a student pencil (#2 HB) is used to draw continuous traces on an

office copy paper for specific cycles (Figure S5), followed by cutting the pencil traces into defined geometry. The drawn pencil traces have good conductivity and can be used to light up an LED bulb (Figure 2f). From the microscopy image (Figure 2g), it is observed that graphite materials are successfully transferred from the rough and porous paper substrate. The electrical resistance of the graphite traces declines significantly during the first two drawing cycles and reaches a relatively low level ($11 \pm 2\text{ k}\Omega/\square$) after the third drawing cycle (Figure 2h). The electrical resistance of the graphite traces also decreases when increasing the trace width (Figure 2i). The enhanced conductivity of the pencil traces with increased drawing cycle can be attributed to the improved density of the conductive graphite networks (Figure S6). For the fabrication of the proposed sensing platform, graphite traces with $\approx 1\text{ mm}$ width and 3 drawing cycles have the desired conductance and are employed for the following study unless otherwise specified.

The structural layouts of the mechanical and thermal sensing devices are illustrated in Figure 2j. Both of these two types of sensing devices are fabricated on a commercial skin-safe double-sided adhesive tape. For the mechanical sensing devices, two

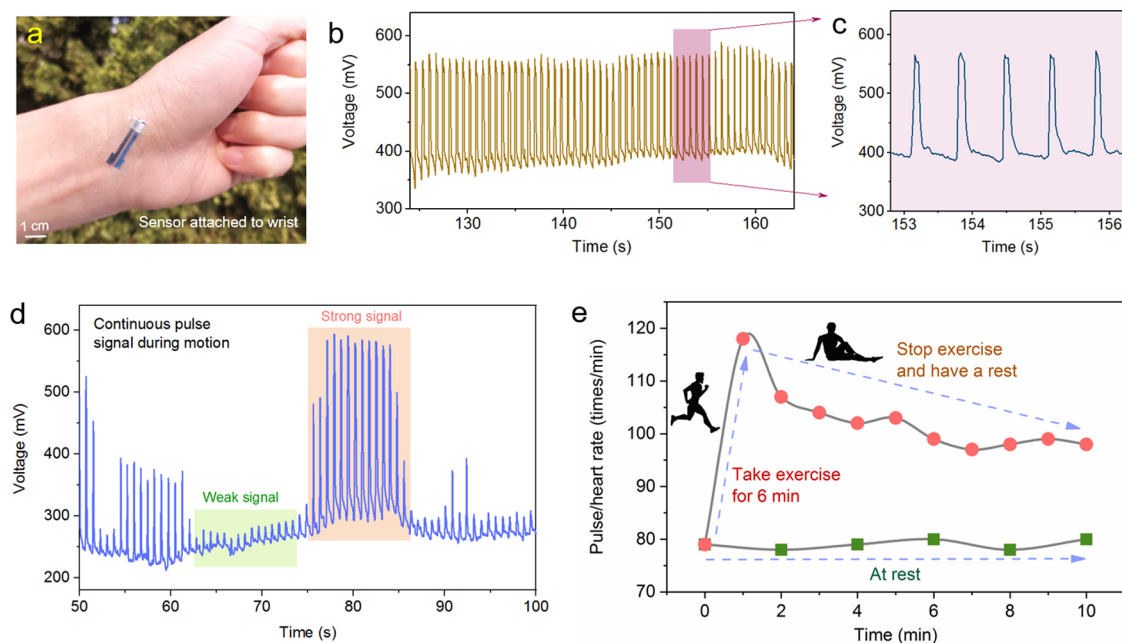


Figure 4. Heart/pulse rate monitoring with home-made mechanical sensors. (a) Photograph showing a flexible mechanical sensor attached to the wrist of the subject. (b and c) Continuously recorded pulse signals with the home-made mechanical sensors, from which the heart rate and pulse rate can be calculated. (d) Continuously recorded pulse signals with motion artifacts. The signal intensity varies due to the motion artifacts, while the pulse peaks can still be clearly recognized. (e) Continuously measured heart/pulse rate of a subject for 10 min when the subject is kept at rest (green squares) and when the subject takes 6 min of exercise and then have a rest (red circles).

spacers are placed between the substrate and the micro-structured electrolyte to normalize the initial device output into zero. For the thermal sensing devices, an H-shaped thin electrolyte film of relatively low Gly content is bridged across the two electrodes. This narrow and thin electrolyte bridge enables us to thermally regulate the internal impedance between the two electrodes efficiently. The assembly and photographs of the final sensors are presented in Figure S7. These proposed sensing devices can be adhered to the skin firmly, even when stretching or squeezing the skin (Figure 2k–m), which is attributed to the intrinsic adhesive property of the tape substrate.

Performance of Home-Made Mechanical/Thermal Sensors. The performance of the home-made mechanical and thermal sensors is shown in Figure 3. When gradually applying an external force on the mechanical sensors, the sensor signal output exhibits a continuous and smooth upswing and reaches a steady state (up to ≈ 900 mV) gradually (Figure 3a), indicating the desirable capability of the sensors in continuous monitoring of mechanical stimulations (Movie S1). The signal output of our proposed sensors is totally self-generated and does not rely on an external power supply, featuring ultralow power consumption.

The response behaviors of the mechanical sensors can be readily regulated via tuning the Gly content in the glue/Gly/NaCl electrolyte. As presented in Figure 3b, mechanical sensors with the electrolyte of a higher Gly content exhibit higher sensitivity and a higher signal output. This is due to the fact that Gly acts as a humectant and can increase the water content and ionic conductivity of the electrolyte.²⁴ Sensors with the glue/Gly/NaCl-32% electrolyte show the highest sensitivity and thus are selected for the following study unless otherwise specified. The effect of the microstructure of the electrolyte on the sensor performance is shown in Figure S8. These home-made mechanical sensors exhibit rapid response and recovery behaviors to the application and release of mechanical

stimulation (Figure 3c), with the response and recovery speeds measured to be ≈ 35 and ≈ 40 ms, respectively. Benefiting from the high response/recovery rates, these mechanical sensors are also qualified to monitor dynamic mechanical stimulations of frequency from 0.1 to 1.6 Hz (Figure 3d). Such a detectable frequency range can cover most of the mechanical variations generated by diverse human physiological activities. Moreover, the sensing behavior of the mechanical sensors remains highly stable in a cyclic test over 1000 cycles, revealing good reproducibility and reliability of our home-made sensors (Figure 3e).

The response behaviors of the home-made thermal sensors are shown in Figure 3f and Movie S2. The sensor signal output increases with temperature because the intrinsic impedance of the glue/Gly/NaCl electrolyte decreases with temperature significantly (Figure S3). It is noticed that thermal sensors with the electrolyte of a higher Gly content exhibit higher sensitivity and a lower temperature detection range. This is because the electrolyte with a higher Gly content has lower intrinsic impedance, which facilitates the output of the potential difference established between the two electrodes (Figure 1d). Thus, we can easily tune the sensing behaviors of the thermal sensors to achieve a desirable sensor sensitivity or temperature detection range. With these home-made thermal sensors, we can continuously monitor the temperature variations ranging from ≈ 20 to ≈ 50 °C, which can fully cover the relevant physiological temperatures and enables monitoring most of the human physiological activities. The response behaviors of the thermal sensors to a warm object (≈ 31 °C) touch and a cold object (≈ 0 °C) touch are shown in Figure 3g,h. Upon the application of a warm stimulation to the device, the sensor signal output exhibits a gradual increase (Figure 3g). In contrast, when applying a cold stimulation to the device, the sensor signal output exhibits a gradual decrease (Figure 3h). After removing the warm or cold objects from the devices, the sensor signals go back to the initial

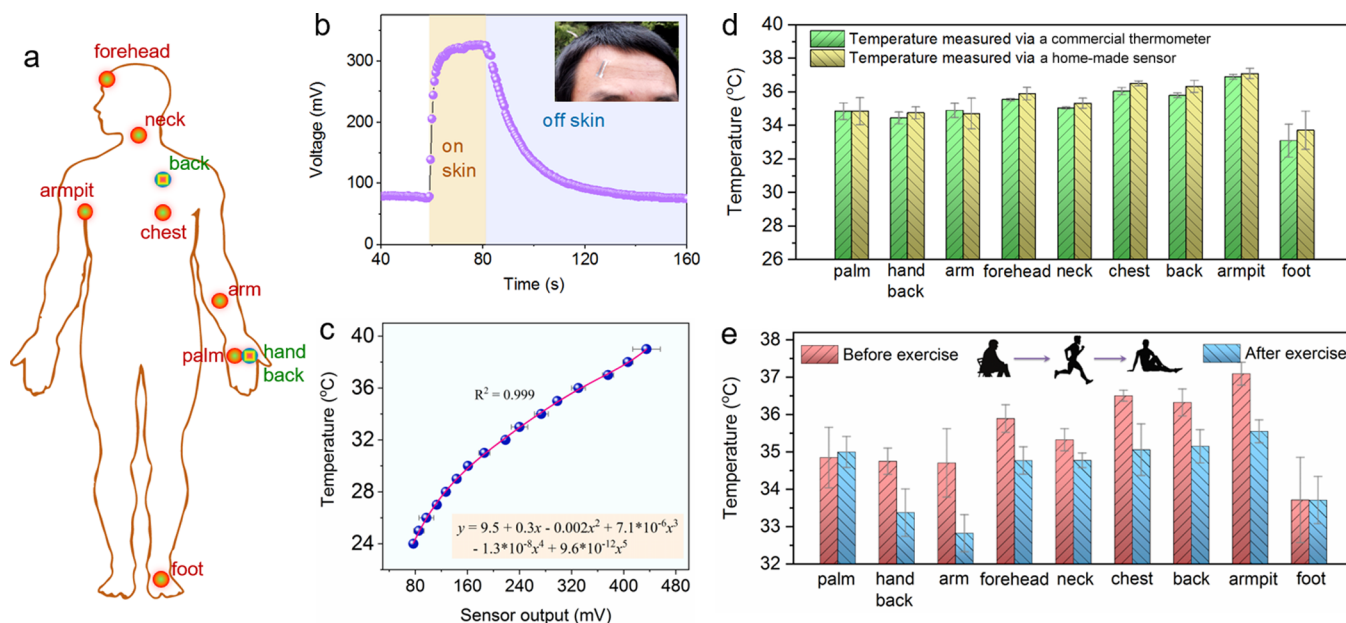


Figure 5. Body temperature monitoring with home-made thermal sensors. (a) Illustration showing the different body positions where the home-made thermal sensors are attached to evaluate the body temperature. (b) Sensor signal variation when a thermal sensor is attached to the body and then removed from the body. (c) Calibration curve of the thermal sensor, which allows us to convert the sensor output to body temperature. (d) Body temperature measured at different body positions with a commercial thermometer and our home-made thermal sensor. (e) Body temperature measured at different body positions before and after the subject takes 6 min of exercise.

level gradually. Interestingly, these home-made thermal sensors have ultrahigh sensitivity and enable us to detect a warm object (Movie S3, Figure S9) or a cold object (Movie S4, Figure S9) in a non-contact sensing style, which can greatly broaden the application range of these thermal sensors in other emerging fields.

A comprehensive comparison of the proposed home-made sensors with other reported sensors in terms of fabrication procedure, necessity of power supply, detectable stimuli, and basic sensor performance is provided in Table S3. In addition, the response stability and durability of the sensors were also investigated and are discussed in Figure S10.

Heart/Pulse Rate Monitoring with Mechanical Sensors. Heart/pulse rate is a critical sign that reflects the dynamic cardiovascular status depending on the emotional state, physical activity, and health status.^{25,26} Here, the feasibility of using our home-made mechanical sensors for continuous heart/pulse rate tracking is evaluated. As shown in Figure 4a, a flexible mechanical sensor is attached to the wrist of a healthy subject (male, 30 years old) to monitor the arterial blood pressure variations in real time. From the recorded arterial pressure waveforms (Figure 4b,c, Movie S5), the heart/pulse rate of this subject can be calculated (≈ 90 beats/min on average) and analyzed continuously. High-quality pulse signals (i.e., signals of high intensity) can be acquired when the sensor is intimately attached to the radial artery of the subject (Figure 4d). Motion artifacts can decrease the intimacy between the sensor and the radial artery and thus reduce the signal amplitude (i.e., weak signal in Figure 4d), which, however, does not affect the acquisition and calculation of the heart/pulse rate of the subject. The validation of pulse monitoring reliability of the home-made sensors was also conducted by using a commercial medical setup (Figure S11).

In addition, we monitor the pulse waveforms of a subject continuously for 10 min in two situations: (1) the subject is kept

at rest (Figure S12a) and (2) the subject first takes some exercise and then stops exercising (Figure S12b). As presented in Figure 4e, when the subject is kept at rest, the calculated heart/pulse rate from pulse waveforms remains nearly constant with ≈ 79 beats/min on average. In contrast, when the subject takes 6 min of exercise, the heart/pulse rate ramps up to 118 beats/min. After the subject stops exercise, the calculated heart/pulse rate exhibits a downtrend and recovers gradually. These results verify that the home-made sensors are qualified for continuous heart/pulse rate tracking.

Body Temperature Monitoring with Thermal Sensors. Precise and continuous monitoring of body temperature is crucial to understand the metabolic and pathological status.^{27–29} Here, we demonstrate that our proposed home-made thermal sensors are qualified for continuously monitoring the body temperature at diverse positions, as illustrated in Figure 5a. Typically, when the sensors are attached to the human body, the signal output of the thermal sensors shows an immediate upswing and then reaches a steady state (Figure 5b). Upon removal from the human body, the sensor signal reverts to its initial value gradually. Through careful calibration of the thermal sensors (Figure 5c), the sensor signal outputs (in mV) at the steady state (i.e., on-skin phase) can be successfully converted into temperature values (in °C) with high accuracy ($R^2 = 0.999$), allowing us to monitor the body temperature continuously.

The epidermal temperature at various body positions of a healthy subject (male, 30 years old) is evaluated with the home-made thermal sensors (Figure S13). The body temperature measured at the palm, hand back, arm, forehead, neck, chest, back, armpit, and foot is 34.9, 34.8, 34.7, 35.9, 35.3, 36.5, 36.3, 37.1, and 33.7 °C, respectively (Figure 5d), which is consistent with that reported in the literature.³⁰ Similar temperature values are also measured with a commercial thermometer, revealing the desirable accuracy and reliability of our home-made thermal sensors. Furthermore, we investigate the body temperature

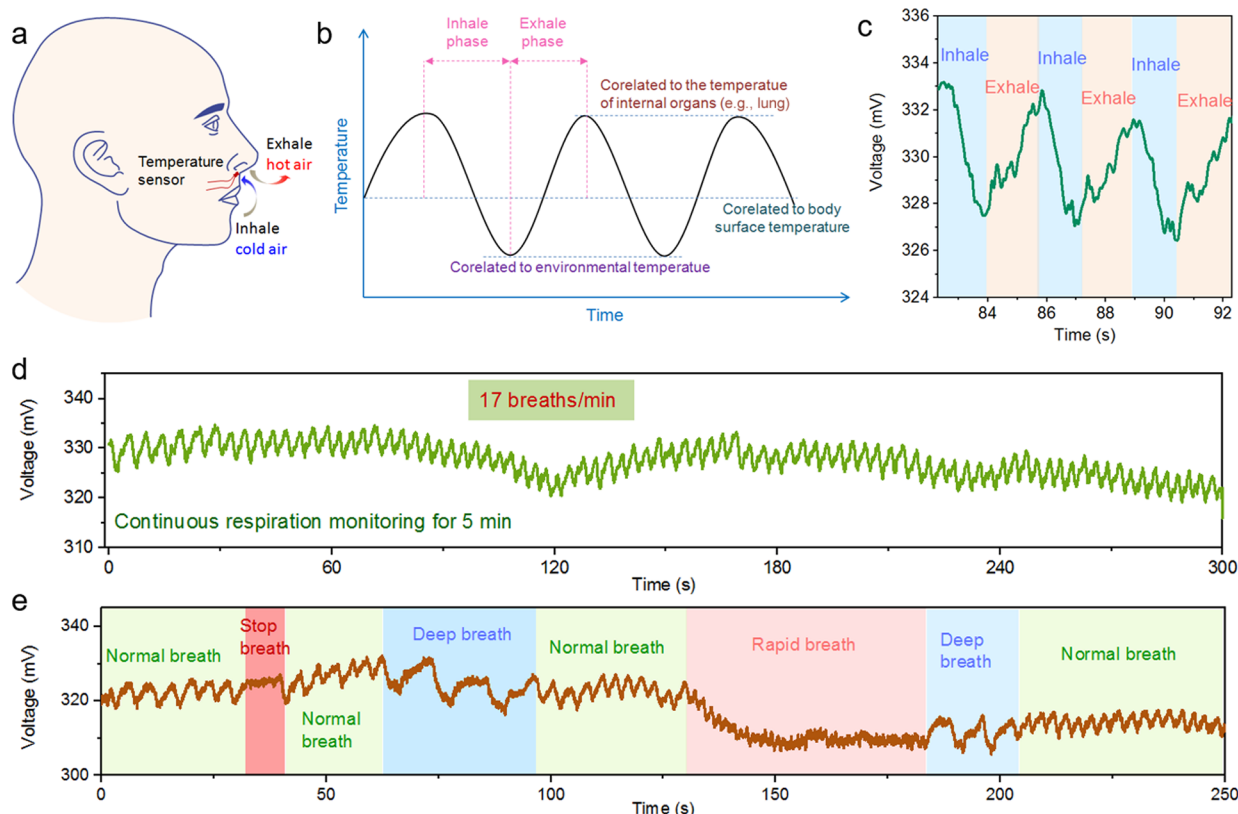


Figure 6. Respiration monitoring with home-made thermal sensors. (a) Schematic showing a home-made thermal sensor attached in front of the nasal cavity to record the temperature variation caused by respiration. (b) Illustration depicting the signal variation of the thermal sensor during respiration and the possible influential factors to the sensor signal output. (c) Typical sensor signal output during respiration (the room temperature is $\approx 24\text{ }^{\circ}\text{C}$). (d) Continuously recorded respiration signal for 5 min, from which an average respiration rate (≈ 17 times/min) can be calculated. (e) Continuously recorded sensor signal in various respiration situations, including normal breath, ceased breath, deep breath, and rapid breath, respectively.

variation of the subject before and after exercise. As presented in Figure 5e, the temperature measured at most body positions shows a decrease after exercise, except for the temperature measured at the palm (shows an increase instead) and the foot (keeps almost unchanged). The decrease in body temperature after exercise can be attributed to the thermal dissipation caused by perspiration and water evaporation, which is commonly reported in the literature.³¹ The slight temperature rise measured at the palm or the temperature invariance measured at the foot might be due to the good thermal insulation (i.e., holding the hand or wearing shoes) or a lack of sweat glands at these positions. These results reveal that the body temperature of diverse positions can be continuously and precisely monitored with our home-made thermal sensors.

Respiration Monitoring with Thermal Sensors. Continuous respiration monitoring is particularly important for the vulnerable population, such as infants, the elderly, and patients with pulmonary diseases (e.g., COVID-19, chronic obstructive pulmonary disease, etc.).^{32,33} Here, we explore the feasibility of using our home-made highly sensitive thermal sensors for continuous respiration monitoring. As shown in Figure 6a, a thermal sensor is attached in front of the nasal cavity to capture small-temperature variations induced by the inhalation and exhalation processes. As illustrated in Figure 6b and shown in Figure 6c, during the inhalation process, the thermal sensor is cooled down by the inhaled air of ambient temperature, and the sensor signal shows a downswing accordingly. On the contrary, in the exhalation process, the thermal sensor is warmed up by the exhaled warm air from the lung, and the sensor signal exhibits an

upswing accordingly. As a demonstration, we record the respiration signal of a healthy subject (male, 30 years old) for 5 min (Figure 6d), from which the respiratory rate (≈ 17 breaths/min) can be easily extracted. To examine the capability of the sensors for detecting/monitoring abnormal respiration situations, the subject is asked to undergo a sequence of different breath situations, including normal breath, stop breath, deep breath, and rapid breath, respectively. As shown in Figure 6e, the whole process can be clearly detected and continuously recorded with our home-made thermal sensors. Specifically, when the subject stops breathing, the sensor signal does not vary obviously and keeps nearly invariable (at a relatively high level). When the subject takes deep breath, the inhalation and exhalation processes are remarkably enhanced in terms of both duration and magnitude. When the subject performs rapid breath, the sensor signal exhibits quick variations and maintains at a relatively low level. In addition to attaching a sensor directly onto the skin near the nasal cavity, the thermal sensor can also be attached to a medical mask for respiration monitoring (Figures S14 and S15), which is more convenient for application.

Respiration and Coughing Monitoring with Mechanical Sensors. In addition to using the home-made thermal sensors for respiration monitoring, we can also use the home-made mechanical sensors for respiration monitoring by tracking the expansion and contraction of the chest. As depicted in Figure 7a, along with the breathing rhythm, the chest cavity expands in the inspiration process and contracts in the expiration process. Tracking the periodic movement of the chest cavity with mechanical sensors allows us to monitor the respiration

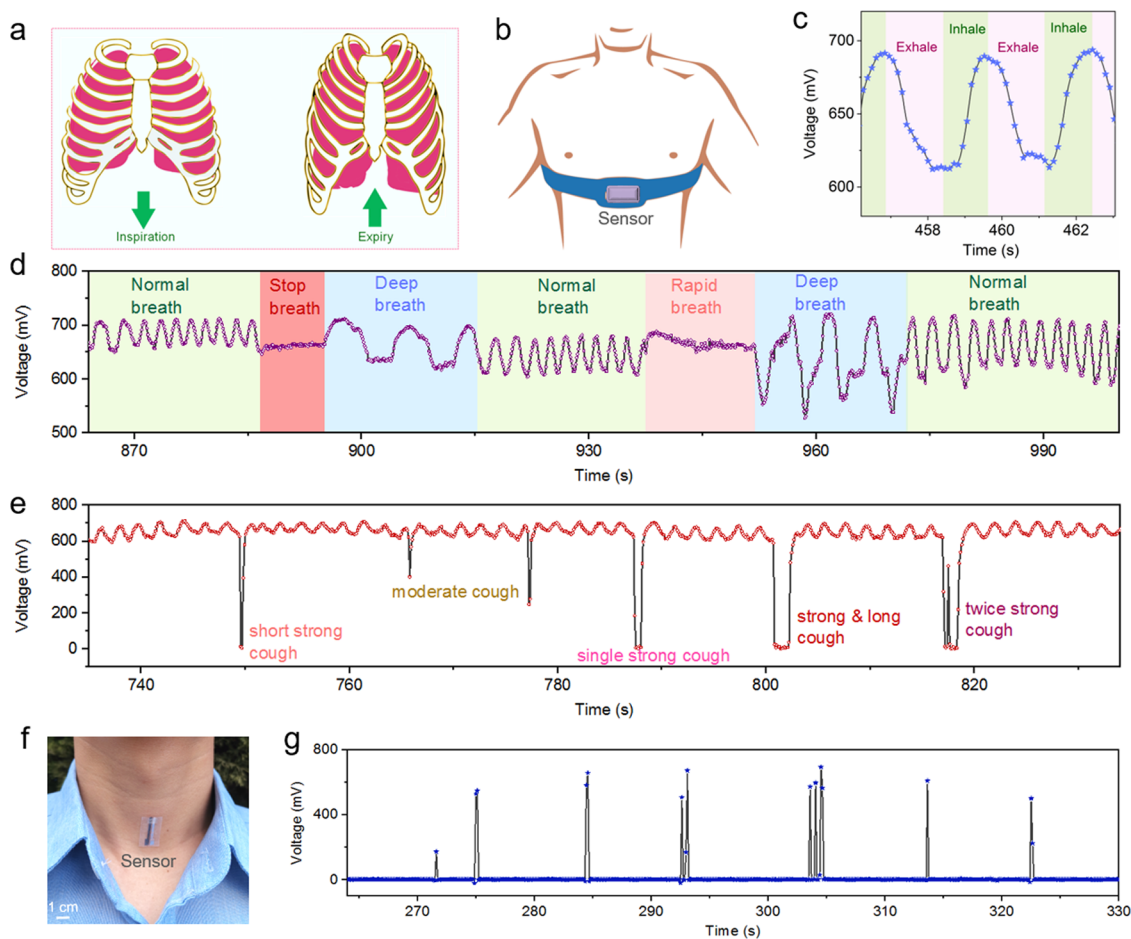


Figure 7. Respiration and coughing monitoring with home-made mechanical sensors. (a and b) Illustrations showing that the respiration process leads to variations in chest volume. Thus, a mechanical sensor can be fixed on the chest to monitor the respiration process. (c) Typical sensor signal output during respiration. (d) Continuously recorded sensor signal during different respiration situations. (e) Continuously recorded sensor signal during various coughing situations. (f and g) Picture and recorded sensor signal when a mechanical sensor is attached to the throat of the subject to monitor the coughing process.

continuously. As illustrated in Figure 7b, a mechanical sensor is fixed to the chest with an elastic belt. During the inhalation process, the chest cavity expands and the pressure applied on the mechanical sensor increases, resulting in an upswing of the sensor signal (Figure 7c). In contrast, during the exhalation process, the chest cavity shrinks and the pressure applied on the sensor decreases, leading to a downswing of the sensor signal. Additionally, a diversity of respiration situations, including normal breath, stop breath, deep breath, and rapid breath, can be monitored and analyzed using this method (Figure 7d). The comparison of respiration monitoring with the home-made mechanical sensors and thermal sensors is presented in Table S4. Also, we compared the respiration monitoring capability and advantages of our sensors with other reported flexible sensors (Table S5).

Moreover, the coughing process of the subject can be detected and tracked in the meantime of respiration monitoring. As verified in Figure 7e, the normal breath process gives rise to a periodic variation in the sensor signal output. Nevertheless, during the coughing process, the sensor signal experiences an abrupt drop, which stems from the quick contraction of the chest cavity. A stronger and longer coughing process leads to signal drops of higher magnitude and longer duration. Multiple consecutive coughs can also be detected in real time. In addition, we can attach a sensor to the throat of the subject to monitor the

coughing process (Figure 7f). The coughing process causes strong vibrations of the throat, which can be tracked for monitoring coughing. As presented in Figure 7g, the sensor signal exhibits abrupt increases during the coughing process, which can be attributed to the compression of the sensor by the throat vibrations. The coughing magnitude and duration can also be reflected in the recorded sensor signal.

In addition to developing a home-made and self-powered sensing platform for the monitoring of diverse vital signs, we contribute a custom-designed circuit board that can be used to collect data from the home-made sensors. Based on the custom-designed circuit, a variety of physiological activities can be detected and monitored in real time, which is fully discussed in Figures S16 and S17.

CONCLUSIONS

In summary, the study presented here demonstrates that wearable electronic sensors that are usually fabricated in the lab via sophisticated and expensive procedures can also be created just using daily necessities and home settings. The proposed home-made sensing platform is totally self-powered, skin-attachable, and highly sensitive to both thermal and mechanical stimulations. The thermal and mechanical sensing modalities have good signal compatibility (i.e., only potential difference output) and thus feature a greatly simplified

operation/measurement. Experimental results show that the home-made sensing platform is well qualified for the precise and continuous monitoring of a wide spectrum of physiological vital signs, such as body temperature, heart/pulse rate, respiratory rate, coughing, and diverse body motions. Compared to the lab-built, expensive, and complicated sensing devices, this proposed home-made sensing platform shows comparable or even superior performance but offers significant advantages in terms of affordability, accessibility, disposability, and energy-efficiency, exhibiting promising applications in home-centered healthcare in low-resource environments. Moreover, this home-made, multifunctional, and powerful sensing platform can serve as a prototype and paradigm for classroom education and clinical training purposes.

■ ASSOCIATED CONTENT

SI Supporting Information

The Supporting Information is available free of charge at <https://pubs.acs.org/doi/10.1021/acssensors.3c00630>.

Experimental section, characterization and measurement, signal generation principle of the sensing system, sensing mechanisms of the mechanical and thermal sensors, microstructure of the electrolyte, characterization of the pencil-drawn graphite electrode, response behaviors of home-made mechanical sensors, non-contact sensing capability of the thermal sensors, performance stability of the mechanical and thermal sensors, pulse signal monitoring with home-made mechanical sensors, body temperature and respiration monitoring with the home-made thermal sensors, monitoring of different physiological activities with a custom-made circuit board, cost calculations of the home-made sensors, comprehensive comparison of the home-made sensors with other reported sensors, and respiration monitoring with home-made mechanical sensors, thermal sensors, and other reported sensors (PDF)

Response behavior of the home-made and self-powered mechanical sensors to a finger touch, where the pressure/force variation caused by the finger touch could be perceived and monitored in real time (MP4)

Response behavior of the home-made and self-powered mechanical sensors to a finger touch, where the temperature variation caused by the gentle finger touch could be detected and monitored in real time (MP4)

Non-contact sensing behavior of the home-made thermal sensors to a warm hand (surface temperature: ≈ 31 °C) approach (≈ 1.5 cm in the minimum distance), demonstrating the ultrasensitive response and non-contact sensing capability of the sensors based on thermal radiation effect (MP4)

Non-contact thermosensation behavior of the home-made thermal sensors to a cold object (surface temperature: ≈ 4 °C) approach (≈ 1.5 cm in the minimum distance), showing the ultrasensitive and non-contact sensing capability of the sensors to cold objects (MP4)

Continuously recorded pulse signal from a human subject with the home-made and self-powered mechanical sensors, from which the pulse/heart rate can be extracted and analyzed (MP4)

■ AUTHOR INFORMATION

Corresponding Authors

Xiaodong Wu – School of Mechanical Engineering, Sichuan University, Chengdu 610065, China; orcid.org/0000-0002-8005-6738; Email: xiaodong_wu@scu.edu.cn

Ana C. Arias – Department of Electrical Engineering and Computer Sciences, University of California, Berkeley, California 94720, United States; orcid.org/0000-0001-6866-5250; Email: acarias@eecs.berkeley.edu

Authors

Wenjuan Ren – School of Mechanical Engineering, Sichuan University, Chengdu 610065, China

Yuhan Wen – Department of Electrical Engineering and Computer Sciences, University of California, Berkeley, California 94720, United States

Seiya Ono – Department of Electrical Engineering and Computer Sciences, University of California, Berkeley, California 94720, United States

Juan Zhu – Department of Electrical Engineering and Computer Sciences, University of California, Berkeley, California 94720, United States; orcid.org/0000-0003-3341-2215

James W. Evans – Department of Materials Science and Engineering, University of California, Berkeley, California 94720, United States

Complete contact information is available at:

<https://pubs.acs.org/doi/10.1021/acssensors.3c00630>

Author Contributions

X.W. designed the project. X.W. designed and conducted the experiments under the supervision of A.C.A. and J.W.E. W.R., Y.W., S.O., and J.Z. contributed to the characterization and discussion. X.W. wrote the manuscript, and all authors read and revised the manuscript.

Funding

This work was supported in part by the Bakar Fellows Program and the National Science Foundation under Grant No. 1610899 and FlexTech Alliance under Grant No. AFOSR 42299. Xiaodong Wu thanks the Sichuan Science and Technology Program (2022YFS0025) and “the Fundamental Research Funds for the Central Universities of China” for the financial support.

Notes

The authors declare no competing financial interest.

■ ACKNOWLEDGMENTS

The authors acknowledge Yangyang Han for helpful discussions.

■ REFERENCES

- (1) Khan, Y.; Ostfeld, A. E.; Lochner, C. M.; Pierre, A.; Arias, A. C. Monitoring of Vital Signs with Flexible and Wearable Medical Devices. *Adv. Mater.* **2016**, *28*, 4373–4395.
- (2) Xu, S.; Jayaraman, A.; Rogers, J. A. Skin sensors are the future of health care. *Nature* **2019**, *571*, 319–321.
- (3) Ray, T. R.; Choi, J.; Bandodkar, A. J.; Krishnan, S.; Gutruf, P.; Tian, L.; Ghaffari, R.; Rogers, J. A. Bio-Integrated Wearable Systems: A Comprehensive Review. *Chem. Rev.* **2019**, *119*, 5461–5533.
- (4) Ha, M.; Lim, S.; Ko, H. Wearable and flexible sensors for user-interactive health-monitoring devices. *J. Mater. Chem. B* **2018**, *6*, 4043–4064.
- (5) Dervisevic, M.; Alba, M.; Prieto-Simon, B.; Voelcker, N. H. Skin in the diagnostics game: Wearable biosensor nano- and microsystems for medical diagnostics. *Nano Today* **2020**, *30*, No. 100828.

- (6) Rogers, J.; Malliaras, G.; Someya, T. Biomedical devices go wild. *Sci. Adv.* **2018**, *4*, No. eaav1889.
- (7) Liu, Y.; Pharr, M.; Salvatore, G. A. Lab-on-Skin: A Review of Flexible and Stretchable Electronics for Wearable Health Monitoring. *ACS Nano* **2017**, *11*, 9614–9635.
- (8) Yang, J. C.; Mun, J.; Kwon, S. Y.; Park, S.; Bao, Z.; Park, S. Electronic Skin: Recent Progress and Future Prospects for Skin-Attachable Devices for Health Monitoring, Robotics, and Prosthetics. *Adv. Mater.* **2019**, *31*, No. e1904765.
- (9) Chu, B.; Burnett, W.; Chung, J. W.; Bao, Z. Bring on the bodyNET. *Nature* **2017**, *549*, 328–330.
- (10) Patel, S.; Park, H.; Bonato, P.; Chan, L.; Rodgers, M. A review of wearable sensors and systems with application in rehabilitation. *J. NeuroEng. Rehabil.* **2012**, *9*, 21.
- (11) Gao, W.; Ota, H.; Kiriya, D.; Takei, K.; Javey, A. Flexible Electronics toward Wearable Sensing. *Acc. Chem. Res.* **2019**, *52*, 523–533.
- (12) Han, S. T.; Peng, H.; Sun, Q.; Venkatesh, S.; Chung, K. S.; Lau, S. C.; Zhou, Y.; Roy, V. A. L. An Overview of the Development of Flexible Sensors. *Adv. Mater.* **2017**, *29*, No. 1700375.
- (13) Matsuhisa, N.; Chen, X.; Bao, Z.; Someya, T. Materials and structural designs of stretchable conductors. *Chem. Soc. Rev.* **2019**, *48*, 2946–2966.
- (14) Lee, S.; Franklin, S.; Hassani, F. A.; Yokota, T.; Nayeem, M. O. G.; Wang, Y.; Leib, R.; Cheng, G.; Franklin, D. W.; Someya, T. Nanomesh pressure sensor for monitoring finger manipulation without sensory interference. *Science* **2020**, *370*, 966–970.
- (15) An, B. W.; Heo, S.; Ji, S.; Bien, F.; Park, J. U. Transparent and flexible fingerprint sensor array with multiplexed detection of tactile pressure and skin temperature. *Nat. Commun.* **2018**, *9*, 2458.
- (16) Jayathilaka, W.; Qi, K.; Qin, Y.; Chinnappan, A.; Serrano-Garcia, W.; Baskar, C.; Wang, H.; He, J.; Cui, S.; Thomas, S. W.; Ramakrishna, S. Significance of Nanomaterials in Wearables: A Review on Wearable Actuators and Sensors. *Adv. Mater.* **2019**, *31*, No. e1805921.
- (17) Yao, S.; Ren, P.; Song, R.; Liu, Y.; Huang, Q.; Dong, J.; O'Connor, B. T.; Zhu, Y. Nanomaterial-Enabled Flexible and Stretchable Sensing Systems: Processing, Integration, and Applications. *Adv. Mater.* **2020**, *32*, No. e1902343.
- (18) Wen, N.; Zhang, L.; Jiang, D.; Wu, Z.; Li, B.; Sun, C.; Guo, Z. Emerging flexible sensors based on nanomaterials: recent status and applications. *J. Mater. Chem. A* **2020**, *8*, 25499–25527.
- (19) Hu, B.; Chen, W.; Zhou, J. High performance flexible sensor based on inorganic nanomaterials. *Sens. Actuators, B* **2013**, *176*, 522.
- (20) Lee, Y.; Kim, J.; Koo, J. H.; Kim, T.-H.; Kim, D.-H. Nanomaterials for bioelectronics and integrated medical systems. *Korean J. Chem. Eng.* **2017**, *35*, 1–11.
- (21) Chun, K. Y.; Son, Y. J.; Jeon, E. S.; Lee, S.; Han, C. S. A Self-Powered Sensor Mimicking Slow- and Fast-Adapting Cutaneous Mechanoreceptors. *Adv. Mater.* **2018**, *30*, No. e1706299.
- (22) Mori, R. Recent Developments for Aluminum–Air Batteries. *Energy Rev.* **2020**, *3*, 344–369.
- (23) Xhanari, K.; Finšgar, M. Organic corrosion inhibitors for aluminum and its alloys in chloride and alkaline solutions: A review. *Arab. J. Chem.* **2019**, *12*, 4646–4663.
- (24) Wu, J.; Wu, Z.; Xu, H.; Wu, Q.; Liu, C.; Yang, B.-R.; Gui, X.; Xie, X.; Tao, K.; Shen, Y.; Miao, J.; Norford, L. K. An intrinsically stretchable humidity sensor based on anti-drying, self-healing and transparent organohydrogels. *Mater. Horiz.* **2019**, *6*, 595–603.
- (25) Fan, X.; Huang, Y.; Ding, X.; Luo, N.; Li, C.; Zhao, N.; Chen, S.-C. Alignment-Free Liquid-Capsule Pressure Sensor for Cardiovascular Monitoring. *Adv. Funct. Mater.* **2018**, *28*, No. 1805045.
- (26) Wang, C.; Li, X.; Hu, H.; Zhang, L.; Huang, Z.; Lin, M.; Zhang, Z.; Yin, Z.; Huang, B.; Gong, H.; Bhaskaran, S.; Gu, Y.; Makihata, M.; Guo, Y.; Lei, Y.; Chen, Y.; Wang, C.; Li, Y.; Zhang, T.; Chen, Z.; Pisano, A. P.; Zhang, L.; Zhou, Q.; Xu, S. Monitoring of the central blood pressure waveform via a conformal ultrasonic device. *Nat. Biomed. Eng.* **2018**, *2*, 687–695.
- (27) Ma, Y.; Choi, J.; Hourlier-Fargette, A.; Xue, Y.; Chung, H. U.; Lee, J. Y.; Wang, X.; Xie, Z.; Kang, D.; Wang, H.; Han, S.; Kang, S. K.; Kang, Y.; Yu, X.; Slepian, M. J.; Raj, M. S.; Model, J. B.; Feng, X.; Ghaffari, R.; Rogers, J. A.; Huang, Y. Relation between blood pressure and pulse wave velocity for human arteries. *Proc. Natl. Acad. Sci. U. S. A.* **2018**, *115*, 11144–11149.
- (28) Shin, J.; Jeong, B.; Kim, J.; Nam, V. B.; Yoon, Y.; Jung, J.; Hong, S.; Lee, H.; Eom, H.; Yeo, J.; Choi, J.; Lee, D.; Ko, S. H. Sensitive Wearable Temperature Sensor with Seamless Monolithic Integration. *Adv. Mater.* **2020**, *32*, No. e1905527.
- (29) Li, Q.; Zhang, L. N.; Tao, X. M.; Ding, X. Review of Flexible Temperature Sensing Networks for Wearable Physiological Monitoring. *Adv. Healthcare Mater.* **2017**, *6*, No. 1601371.
- (30) Bierman, W. The Temperature of the Skin Surface. *JAMA* **1936**, *106*, 1158–1162.
- (31) Nadel, E. R.; Bullard, R. W.; Stolwijk, J. A. Importance of skin temperature in the regulation of sweating. *J. Appl. Physiol.* **1971**, *31*, 80–87.
- (32) Su, Y.; Chen, G.; Chen, C.; Gong, Q.; Xie, G.; Yao, M.; Tai, H.; Jiang, Y.; Chen, J. Self-Powered Respiration Monitoring Enabled By a Triboelectric Nanogenerator. *Adv. Mater.* **2021**, *33*, No. e2101262.
- (33) Pang, Y.; Jian, J.; Tu, T.; Yang, Z.; Ling, J.; Li, Y.; Wang, X.; Qiao, Y.; Tian, H.; Yang, Y.; Ren, T. L. Wearable humidity sensor based on porous graphene network for respiration monitoring. *Biosens. Bioelectron.* **2018**, *116*, 123–129.